LA-8418-PR

Progress Report

C.3

Applied Nuclear Data Research and Development

January 1—March 31, 1980

LOS ALAMOS SCIENTIFIC LABORATORY
Post Office Box 1663 Los Alamos, New Mexico 87545

The four most recent reports in this series, unclassifed, are LA-7843-PR, LA-8036-PR, LA-8157-PR, and LA-8298-PR.

This report was not edited by the Technical Information staff.

This work was performed under the auspices of the US Department of Energy's Office of Military Application, Division of Reactor Research and Technology, Office of Basic Energy Sciences, and Office of Fusion Energy; and the Electrical Power Research Institute.

UNITED STATES
DEPARTMENT OF ENERGY
CONTRACT W-7405-ENG. 36

LA-8418-PR
Progress Report

UC-34c
Issued: June 1980

Applied Nuclear Data Research and Development

January 1—March 31, 1980

Compiled by

C. I. Baxman and P. G. Young

CONTENTS

APPLIED NUCLEAR DATA RESEARCH AND DEVELOPMENT
QUARTERLY PROGRESS REPORT
January 1 - March 31, 1980

Compiled by

C. I. Baxman and P. G. Young

ABSTRACT

This progress report describes the activities of the Los Alamos Nuclear Data Group for the period January 1, 1980, through March 31, 1980. The topical content is summarized in in the contents.

I. THEORY AND EVALUATION OF NUCLEAR CROSS SECTIONS

A. Representation of Charged-Particle Elastic Cross Sections (G. Hale and D. C. Dodder

Charged-particle elastic cross sections are increasingly of interest in fusion applications where realistic calculations of the slowing down of projectile ions (or the knock-on excitation of the recoil ions) are desired. We are studying ways of representing charged-particle elastic cross sections over the full angular range which could be used to tabulate the calculated cross sections available from our R-matrix analyses of light systems.

In the case of distinguishable particles, the cross section can be expanded as

$$\sigma(z) = \sigma_c(z) - \frac{2\eta}{k^2(1-z)} \mathrm{Re}\left[e^{i\eta\ell n\ 1/2(1-z)} \sum_{\ell=0}^{\ell_{mx}} a_\ell P_\ell(z)\right] + \sum_{L=0}^{2\ell_{mx}} b_L P_L(z) \quad , \quad (1)$$

where σ_C is the Rutherford scattering cross section that depends on $z = \cos\theta$, the Coulomb parameter η, and the center-of-mass wave number k; a_ℓ and b_L are expansion coefficients, and ℓ_{mx} is the highest partial wave contributing to the

amplitudes. The a_ℓ are complex numbers since they are sums of scattering amplitudes in the Coulomb-nuclear interference term, while the b_L are real numbers coming from the squared moduli of the amplitudes that form the pure nuclear scattering cross section. The fact that the a_ℓ and b_L are not independent appears to prevent them from being determined reliably from direct fits to experimental data; rather, the nuclear amplitudes are first determined by data fitting, and the expansion coefficients are derived from the amplitudes.

An alternative expansion suitable for direct fits to experimental data results from neglecting the z-dependence of the phase $\phi = \ell n\ 1/2\ (1-z)$ and removing the singularities at z = 1 in Eq. (1) to obtain the expansion

$$(1-z)\ (\sigma-\sigma_C) \approx \sum_{L=0}^{L_{mx}} d_L\ P_L\ (z) \quad , \tag{2}$$

where one expects L_{mx} to be approximately $2\ell_{mx} + 1$. This type of expansion, first proposed by Devaney and Stein,[1] clearly deviates from the exact expression at small angles ($z \to 1$) where ϕ is strongly z-dependent as it approaches $-\infty$, producing infinitely many oscillations in $(1-z)\ (\sigma-\sigma_C)$. This effect is quite pronounced at low energies as is illustrated in Fig. 1, where Eqs. (1) and (2) are compared for the p-^{3}He cross section at 100 keV. Although it is unlikely that these oscillations are of any practical consequence in, for instance, the integral quantities calculated by Perkins and Cullen[2] for elastic scattering of light ions, we are checking this possibility.

B. Calculation of Neutron Cross Sections on Excited State Targets (E. D. Arthur)

Cross sections for neutron reactions on yttrium targets existing in excited states have been calculated in the incident energy range between 0.001 and 20 MeV. The metastable states considered as targets are listed below.

Target	E_x (MeV)	$t_{1/2}$
^{87m}Y	0.3811	13 hours
^{88m1}Y	0.3929	300 microseconds
^{88m2}Y	0.6746	13.9 milliseconds
^{89m}Y	0.9092	16.1 seconds

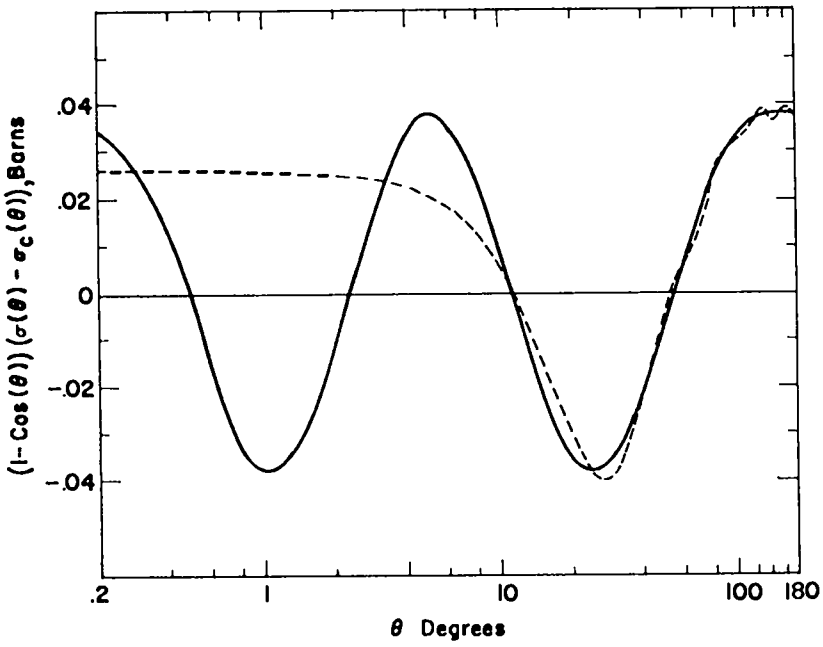

Fig. 1.
Comparison of expansion 2 (dashed curve) to the exact expansion 1 (solid curve) for the quantity $(1-z)(\sigma-\sigma_c)$. Here, σ is the p-^{3}He cross section at 100 keV calculated from a LASL R-matrix analysis.

For each of these target states, all major reactions listed in Table I have been calculated using the parameters and techniques employed in earlier calculations on yttrium and zirconium isotopes as described in Ref. 3.

Because of the spin and, to a lesser degree, energy differences, cross sections calculated for a given excited-state target can be quite different from those calculated for a target existing in its ground state. Figure 2 compares (n,2n) cross sections calculated for ^{88g}Y ($J^\pi = 4^-$, solid curve) to (n,2n) cross sections calculated for ^{88m1}Y ($J^\pi = 1^+$, short dashed curve) and ^{88m2}Y ($J^\pi = 8^+$, long dashed curve) target states. The smaller initial spin of the ^{88m1}Y target state (relative to ^{88g}Y) results in an increased (n,2n) cross section below 17.5 MeV. The (n,2n) cross section for the ^{88m}Y target has a much lower value owing mainly to the higher spin of this state. Figure 3 shows a similar dependence for the calculated (n,p) cross section below 10 MeV. The low-energy capture cross sections shown in Fig. 4 also exhibit a dependence on target state, but in this case the main effect arises from competition from other reactions [(n,p) in the case of the ^{88m1}Y target and (n,n')^{88g}Y in the case of ^{88m2}Y].

TABLE I

Q-VALUES AND THRESHOLDS FOR YTTRIUM EXCITED STATE TARGETS

MAT	MT	Reaction	Q (MeV)	E_{th} (MeV)	Final State
1397	2	$^{87m}Y(n,n')^{87m}Y$	0.00	0.00	1
	16	$^{87m}Y(n,2n)^{86}Y$	-11.458	11.59	0
	16	$^{87m}Y(n,2n)^{86m}Y$	-11.677	11.81	2
	28	$^{87m}Y(n,np+n,pn)^{86}Sr$	- 5.403	5.467	0
	50	$^{87m}Y(n,n'+n,n'\gamma)^{87g}Y$	0.381	0.00	0
	51	$^{87m}Y(n,n'\gamma)^{87m}Y$	- 1.177	1.191	1
	102	$^{87m}Y(n,\gamma)^{88}Y$	9.743	0.00	0
	102	$^{87m}Y(n,\gamma)^{88m1}Y$	9.351	0.00	2
	102	$^{87m}Y(n,\gamma)^{88m2}Y$	9.069	0.00	3
	103	$^{87m}Y(n,p)^{87}Sr$	3.025	0.00	0
	103	$^{87m}Y(n,p)^{87m}Sr$	2.637	0.00	1
	107	$^{87m}Y(n,x\alpha)$	2.772	0.00	0
2398	2	$^{88m1}Y(n,n')^{88m1}Y$	0.00	0.00	2
	16	$^{88m1}Y(n,2n)^{87}Y$	- 8.97	9.072	0
	16	$^{88m1}Y(n,2n)^{87m}Y$	- 9.35	9.458	1
	28	$^{88m1}Y(n,np+n,pn)^{87}Sr$	- 6.325	6.398	0
	28	$^{88m1}Y(n,np+p,pn)^{87m}Sr$	- 6.714	6.791	1
	50	$^{88m1}Y(n,n'+n,n'\gamma)^{88g}Y$	0.393	0.00	0
	52	$^{88m1}Y(n,n'\gamma)^{88m1}Y$	- 0.314	0.3175	2
	53	$^{88m1}Y(n,n'\gamma)^{88m2}Y$	- 0.282	0.285	3
	102	$^{88m1}Y(n,\gamma)^{89}Y$	11.862	0.00	0
	102	$^{88m1}Y(n,\gamma)^{89m}Y$	10.95	0.00	1
	103	$^{88m1}Y(n,p)^{88}Sr$	4.788	0.00	0
	107	$^{88m1}Y(n,x\alpha)$	3.90	0.00	0
3398	2	$^{88m2}Y(n,n')^{88m2}Y$	0.00	0.00	3
	16	$^{88m2}Y(n,2n)^{87}Y$	- 8.688	8.787	0
	16	$^{88m2}Y(n,2n)^{87m}Y$	- 9.069	9.173	1
	28	$^{88m2}Y(n,np+n,pn)^{87}Sr$	- 6.044	6.113	0
	28	$^{88m2}Y(n,np+n,pn)^{87m}Sr$	- 6.432	6.506	1
	50	$^{88m2}Y(n,n'+n,n'\gamma)^{88g}Y$	0.6746	0.00	0
	52	$^{88m2}Y(n,n'\gamma)^{88m1}Y$	0.2817	0.00	2
	53	$^{88m2}Y(n,n'\gamma)^{88m2}Y$	- 0.404	0.4086	3
	102	$^{88m2}Y(n,\gamma)^{89}Y$	12.145	0.00	0
	102	$^{88m2}Y(n,\gamma)^{89m}Y$	11.234	0.00	1
	103	$^{88m2}Y(n,p)^{88}Sr$	5.0695	0.00	0
	107	$^{88m2}Y(n,x\alpha)$	4.182	0.00	0
1399	2	$^{89m}Y(n,n')^{89m}Y$	0.00	0.00	1
	16	$^{89m}Y(n,2n)^{88}Y$	-10.559	10.679	0
	16	$^{89m}Y(n,2n)^{88m1}Y$	-10.952	11.077	2
	16	$^{89m}Y(n,2n)^{88m2}Y$	-11.234	11.362	3
	28	$^{89m}Y(n,np+n,pn)^{88}Sr$	- 6.165	6.235	0
	50	$^{89m}Y(n,n'+n,n'\gamma)^{89g}Y$	0.902	0.00	0
	51	$^{89m}Y(n,n'\gamma)^{89m}Y$	- 1.313	1.328	1
	102	$^{89m}Y(n,\gamma)^{90}Y$	7.766	0.00	0
	102	$^{89m}Y(n,\gamma)^{90m}Y$	7.084	0.00	2
	103	$^{89m}Y(n,p)^{89}Sr$	0.199	0.00	0
	107	$^{89m}Y(n,x\alpha)$	1.598	0.00	0

TABLE I (cont)

NOTES

1. A final state of 0 for reactions specifed by MT=16, 28, 102, 103, or 107 means that the cross section given is the total for that reaction. If the final state is not equal to zero, then the cross section listed is that for population of the given final state.

2. A value, MT=2, means population of the target state by elastic scattering while the population of the target state by gamma-decay of higher states produced in inelastic scattering is denoted (as applicable) by MT=51, 52, or 53.

3. MT=50 means population of the ground state directly by inelastic scattering off the excited target state and by gamma-decay of higher excited states. This does not include gamma-decay of the isomeric target state to the ground state since this occurs on a long time scale, relative to the nuclear processes. At an appropriate time, if the total population of the ground state is desired, then MT=2, 50, and 51, 52, 53 (where applicable) should be added.

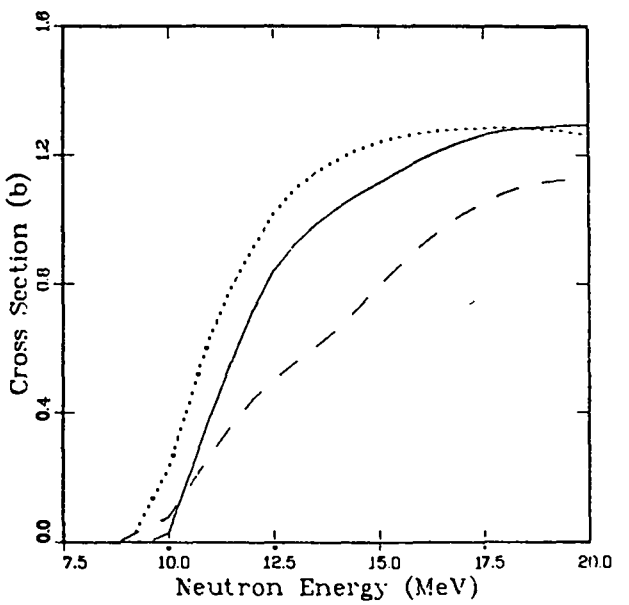

Fig. 2.
Calculated (n,2n) cross sections for ^{88}Y existing as a target in its ground state (solid curve) and its first and second metastable states (short and long dashed curves, respectively).

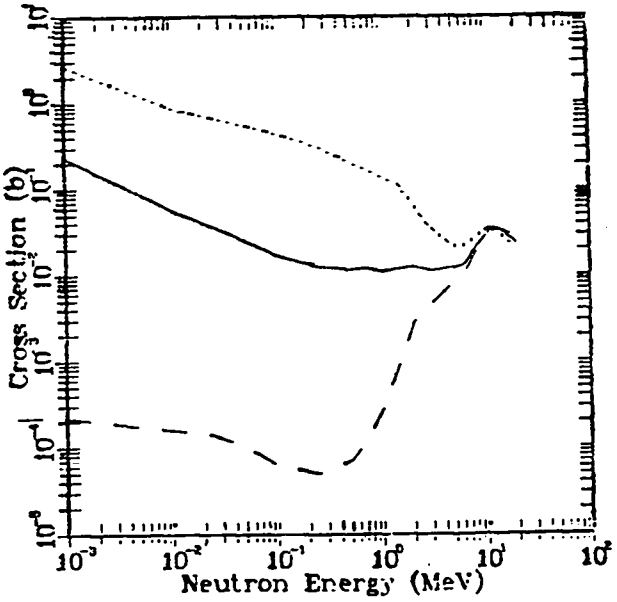

Fig. 3.
Same as Fig. 2 but with $^{88}Y(n,p)$ cross sections.

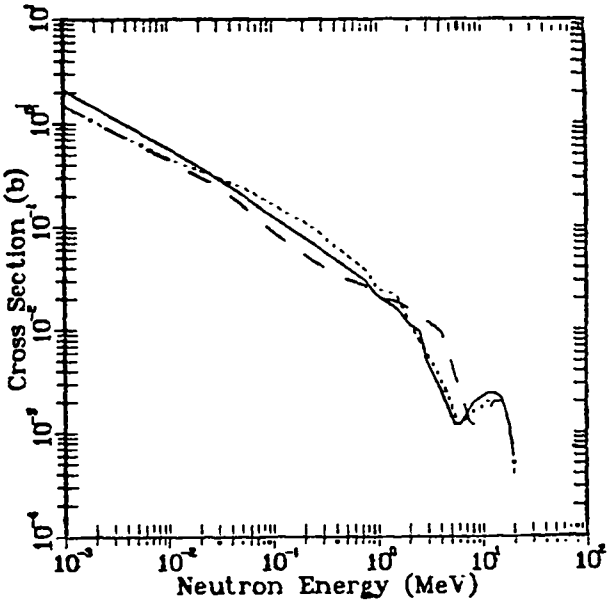

Fig. 4.
^{88g}Y and $^{88m1,88m2}Y$ capture cross sections. The curve labels are the same as Figure 2.

These results indicate that where excited state target cross sections are of interest, significant differences may exist between ground and excited state target results if large spin differences are present.

C. n + Gallium Evaluation (P. G. Young, R. E. MacFarlane, and R. B. Kidman)

Because gallium is present in small amounts in certain fast critical benchmark experiments, it is desirable to include it in benchmark calculations. At present gallium is not among the materials in Version V of ENDF/B. To remedy this situation, we have updated a Lawrence Livermore Laboratory (LLL) evaluation[4] to better represent the available experimental data and have converted it to ENDF/B format. Changes were made in the total cross section, given in Figs. 5 and 6, to better describe the Walt[5] data below 3 MeV and the Foster[6] results at higher energies. The Ga (n,2n) cross section was modified to agree with a measurement by Frehaut,[7] as shown in Fig. 7.

The gallium results have been processed into a 70-group fast-reactor data library and distributed to several laboratories. As noted in Sec. II. B, the effect of putting this evaluation into calculations of the JEZEBEL benchmark experiment is to raise its eigenvalue by 0.0039.

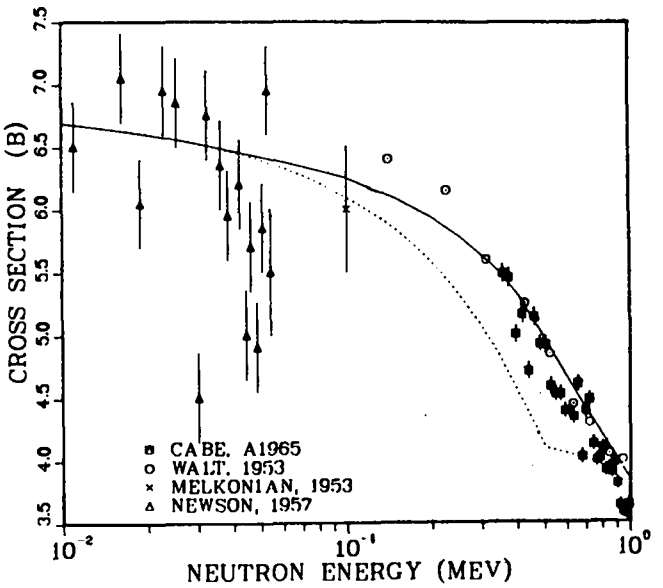

Fig. 5.
Gallium total cross section from 0.01-1.0 MeV. The solid and dashed curves are the LASL and ENDL-78 (Ref. 4) evaluations, respectively. The experimental data are described in Ref. 8.

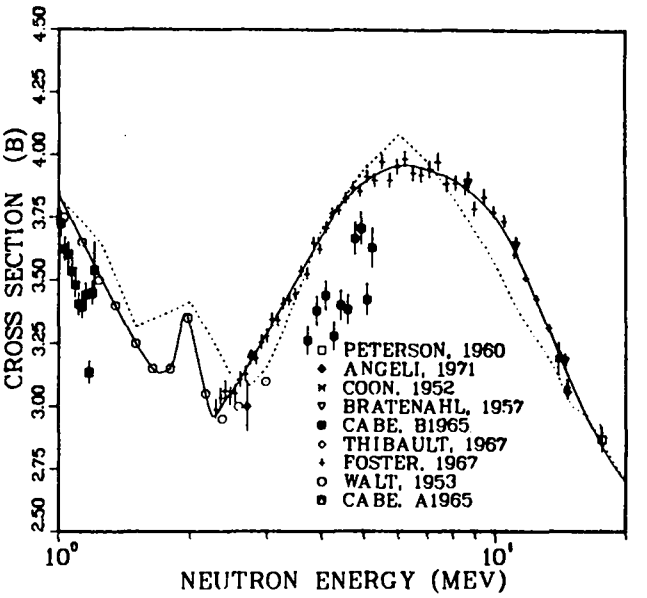

Fig. 6.
Gallium total cross section from 1-20 MeV. The solid and dashed curves are the LASL and ENDL-78 (Ref. 4) evaluations, respectively. The experimental data are described in Ref. 8.

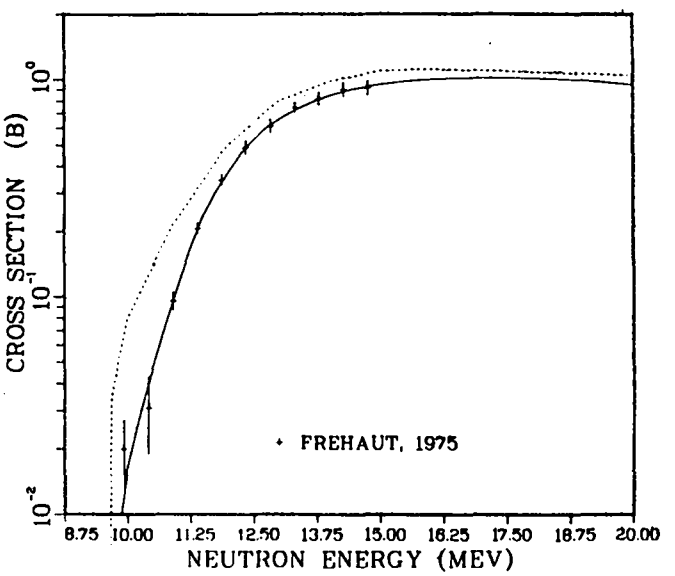

Fig. 7.
Gallium (n,2n) cross sections from threshold to 20 MeV. The solid and dashed curves are the LASL and ENDL-78 (Ref. 4) evaluations, respectively. The experimental data are from Ref. 7.

D. Calculation of Prompt Fission Neutron Spectra and $\bar{\nu}_p$ [D. G. Madland and J. R. Nix (T-9)]

1. Status of Calculations. Contributions due to multiple-chance fission have been included in the calculation of both the prompt fission neutron spectrum and the average prompt fission neutron multiplicity $\bar{\nu}_p$. At high excitation energy of the fissioning nucleus, we include contributions from second-chance (n,nf) fission and third-chance (n,2nf) fission by calculating both the energy spectrum of the neutrons evaporated prior to multiple-chance fission and, if the residual nucleus fissions, the neutron energy spectrum from that fission. Our results obtained with the inclusion of multiple-chance fission processes are described in Ref. 9, and the calculations are completely detailed in Ref. 10.

Calculations of prompt-fission neutron spectra and $\bar{\nu}_p$ have been completed and compared to experimental data for several cases of neutron-induced and spontaneous fission. These results, together with a complete description of the theoretical method, numerical technique, and various physical approximations to the theory, are presented in Ref. 10. An example of our results is shown in Figs. 8 and 9 for the fission of ^{235}U induced by 0.53-MeV neutrons. The experimental data are those of Johansson and Holmqvist[11] and the theoretical calculations are for the two cases of a constant and an energy-dependent cross section for the inverse process of compound-nucleus formation. Results obtained for the two assumptions agree well with the experimental data although there is a clear preference for the calculation with the energy-dependent cross section generated using the Becchetti-Greenlees optical-model potential.[12]

2. Status of Computer Codes. The code FISPOK, which calculates the prompt fission neutron spectrum, its moments, and $\bar{\nu}_p$ for constant compound-nucleus formation cross sections, and the code GTLTLT, which calculates the same quantities for energy-dependent formation cross sections, have been merged into a single code FISPEK. The code FISPEK also calculates Watt and Maxwellian distributions together with their first moments.

A utility code NORM has been written that converts unnormalized experimental prompt fission neutron time-of-flight spectra into normalized energy spectra. The code also converts unnormalized experimental energy spectra into normalized energy spectra. Relativistic corrections and bin-width corrections are available options and the first moment of the normalized experimental spectrum is computed. The most useful option of the utility is the normalization of the

experimental spectrum subject to the constraint that the integral of the normalized experimental spectrum over the energy range of the experiment is equal to the integral of any given theoretical spectrum over the same energy range. This feature of NORM is used to compare experiment and theory in our work.

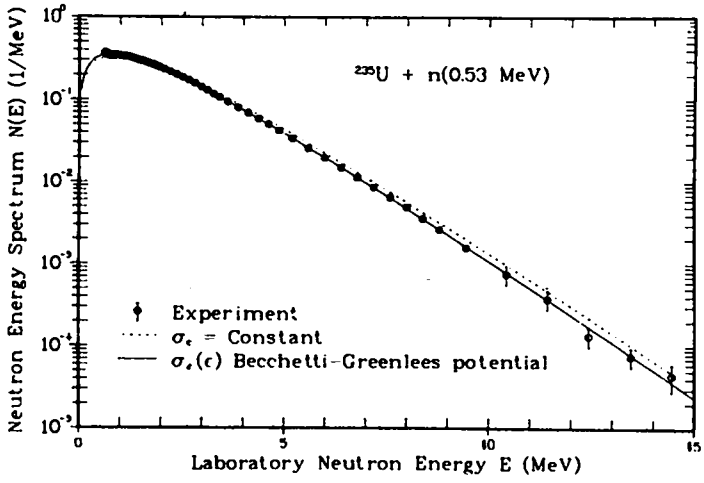

Fig. 8.
Prompt fission neutron spectrum for the fission of ^{235}U induced by 0.53-MeV neutrons. The experimental data are from Ref. 11 and the optical-model potential is from Ref. 12. The theoretical curves are discussed in the text.

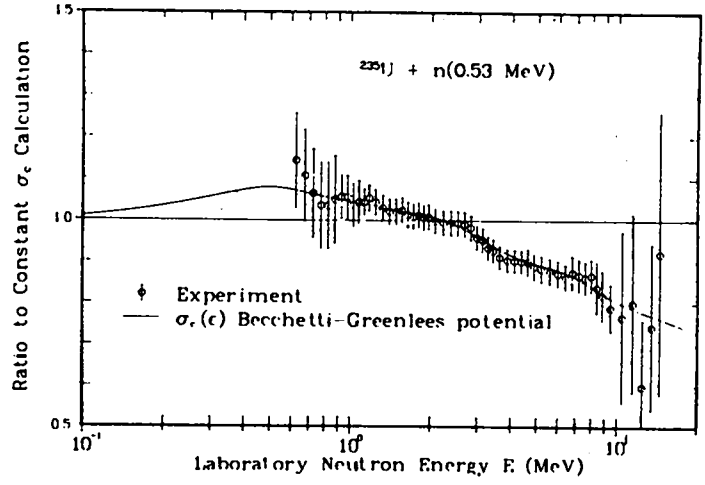

Fig. 9.
Ratios of the energy-dependent prompt fission neutron spectrum calculation and experimental data of Fig. 8 to the constant cross-section fission spectrum calculation of Fig. 8. The theoretical calculations are discussed in in the text.

II. NUCLEAR CROSS SECTION PROCESSING

A. ENDF/B Processing (R. B. Kidman)

An additional 50 ENDF/B-V materials have been processed into a number of standard formats and files that are required by various physics computer codes. In particular, 70-group ISOTXS and BRKOXS files for these 50 materials have been combined with 43 previously generated materials to form a rather complete 93-isotope, 70-group library based on ENDF/B-V data. This library has been sent to Combustion Engineering, Westinghouse Advanced Reactor Division, and General Electric.

B. LASL Benchmarks (R. B. Kidman)

New and revised benchmark specifications were received this quarter for nine Los Alamos Scientific Laboratory (LASL) critical assemblies. Each of these spherical benchmarks was computed using P_3, S_{16} transport theory and the 93-isotope 70-group library mentioned in Sec. II. A. The resulting eigenvalues and three central reaction rate ratios are shown in Table II.

Two trends are evident. First, the fission ratio comparisons to experiment in ^{239}Pu-driven systems are lower than those in ^{235}U-driven systems: approximately 12, 10, and 3% lower, respectively, for the $\sigma_f^{U\text{-}238}/\sigma_f^{U\text{-}235}$, $\sigma_f^{Np\text{-}237}/\sigma_f^{U\text{-}235}$ and $\sigma_f^{U\text{-}239}/\sigma_f^{U\text{-}235}$ ratios. Second, if one temporarily ignores JEZEBEL, the reflected benchmark eigenvalues are predicted approximately 1.2% higher than the bare benchmark eigenvalues.

The results of Table II were computed with infinitely dilute cross sections. The identified trends, especially the eigenvalue trend, suggest that the use of self-shielded cross sections might help. It should be noted, however, that previous calculations with the bare benchmarks JEZEBEL and GODIVA produced insignificant changes when self-shielded cross sections were employed.

When comparing calculated spectra with experimental spectra, it appears that plutonium-driven systems are calculated too soft while uranium-driven systems are calculated too hard. This fits in with the fission ratio trend noted above and suggests that perhaps plutonium and uranium transfer cross sections are not equally good.

The revised JEZEBEL specifications now contain gallium (see Sec. I. D). It is interesting to note that the presence of gallium raises the eigenvalue by 0.0039.

TABLE II

LASL BENCHMARKS (C/E)

Benchmark	K	$\sigma_f^{U\text{-}238}/\sigma_f^{U\text{-}235}$	$\sigma_f^{Np\text{-}237}/\sigma_f^{U\text{-}235}$	$\sigma_f^{Pu\text{-}239}/\sigma_f^{U\text{-}235}$
JEZEBEL	1.0094	0.9250	0.9882	0.9717
GODIVA	1.0013	1.0350	1.0590	0.9932
JEZEBEL-23	0.9947	1.0043	1.0169	
BIGTEN	1.0116	1.0786	1.1338	1.0066
JEZEBEL-PU	1.0008	0.9330	1.0172	
FLATTOP-25	1.0092	1.0336	1.0785	0.9995
FLATTOP-PU	1.0119	0.9307	1.0038	
FLATTOP-23	1.0055	0.9882	1.0241	
THOR	1.0152	0.9247	0.9599	

C. Photonuclear Cross Sections for ENDF/B (R. E. MacFarlane)

A program has been started in collaboration with R. E. Seamon of LASL Group X-6 (Monte-Carlo transport) to create files of photonuclear cross sections for the U. S. ENDF/B files. Such files would be useful in studying effects in high-gamma fields, including dosimetry, transmutation, radiation damage, and nuclear heating. The project divides naturally into three parts: evaluation, processing, and application.

Several collections of photonuclear data presently exist, notably, the Photonuclear Data Center at the National Bureau of Standards (NBS) and the compendium of Berman.[13] Cross sections including photofission (γ,f) and photoparticle production [e.g., (γ,n), (γ,2n), (γ,np)] are available for many isotopes, but angle-and-energy distribution data are rare. As in neutron evaluation, experimental data will have to be supplemented and extended by nuclear-model calculations and the evaluator's instinct.

Photofission will be the easiest to handle. The recent work of Nix and Madland[14] provides well-founded methods to obtain photofission yields ($\bar{\nu}$) and energy distributions of fission neutrons. Such results could be easily obtained in the course of our current program for improving the fission data in ENDF/B. Energy spectra for reactions like (γ,2n) could be obtained using methods typical of neutron evaluations 10 years ago; for example, using a Maxwellian evaporation spectrum with a temperature obtained from level-density systematics. With somewhat more work, a modern statistical-model code such as GNASH[15] could be adapted

to produce the needed data. This approach has the advantage of accounting for many possible exit channels at once while preserving conservation of energy explicitly. For lighter nuclides where statistical models begin to fail, R-matrix codes like EDA[16] can be used, but improvements to allow three-body reactions will be needed.

The key to processing photonuclear data to make it available for application is a data format. At a recent meeting of a subcommittee of the Cross Section Evaluation Working Group (CSEWG) that develops the ENDF/B libraries, we presented a trial format for photonuclear data that is consistent with the existing formats. However, the new format has an important extension; it allows the evaluator to include fractional yields and energy distributions for each possible exit channel of a photonuclear reaction in one file [i.e., (γ,n) + $(\gamma,2n)$ + (γ,np) + ...]. Since this format is very similar to the one used for neutron reactions, it should be straightforward to adapt existing processing codes to handle the new data type.

Data for application should be available in the form of multigroup or continuous energy cross sections for simple transmutation and dosimetry calculations and as complete gamma-particle transfer tables for problems where coupled transport of several particles is needed for an accurate analysis. Such data would fill in the missing quadrant in current coupled neutron-photon transport tables. Some existing multigroup formats and transport codes are already suitable for this purpose.

The direction this photonuclear data program takes and its rate of progress will depend strongly on feedback from potential users with regard to important applications, reactions, and isotopes.

D. Multi-Body Reactions for ENDF/B (R. E. MacFarlane)

The existing ENDF/B formats are quite suitable for reactions that can be described using two-body kinematics such as (n,n') or (n,γ). It is only necessary to specify the cross section (in File 3) and the angular distribution of the secondary particle (in File 4). At higher energies, however, we begin to see additional emitted particles [e.g., (n,2n), (n,n'p)]. Such high-energy reactions are very important for radiotherapy dose calculations, the calculation of neutron transport in fusion devices, and the analysis of radiation damage (especially in support of FMIT, the new Fusion Materials Irradiation Test Facility). For these problems, it will be necessary to supply coupled energy-and-

angle distributions for the neutrons and all the charged particles produced by a reaction; the current assumption of separability of angle and energy (i.e., File 4 and File 5) will not be adequate.

Unfortunately, data this complete are rarely available directly from experiment. In modern evaluation practice, nuclear-model codes are used to smooth and extend experimental data. A recent example is the use of the preequilibrium statistical-model code GNASH[15] coupled with the angular distribution systematics of Kalbach and Mann[17] to produce cross sections and particle distributions for iron between 1 and 40 MeV.[18] The current ENDF/B formats do not allow this wealth of results to be passed on for ultimate application.

Furthermore, for tissue damage associated with particle-beam cancer therapy, material radiation damage, and nuclear-heating calculations, it is useful to have good energy-and-angle distributions for the residual nucleus of a reaction. Such distributions can be computed from the detailed population increments computed by GNASH if possible correlations between the angles of particle emission are neglected. Once again, these useful results cannot be saved in ENDF/B format.

For these reasons, we have developed a new File 6 format for coupled energy-and-angle distributions and proposed it to the Cross Section Evaluation Working Group (CSEWG), which develops the ENDF/B libraries. The format is closely based on a non-standard version of File 6 used in the NJOY cross-section processing code for thermal neutron scattering, so many of the techniques needed to process the new file already exist. It allows for separate distributions and yields for each secondary particle produced by a reaction. The particles are identified by their Z and A, so there is no problem representing residual nuclei or even mesons. A number of different angular representations will be allowed, and either center-of-mass or laboratory coordinates can be used.

We are currently in the process of developing a utility code to extract the particle spectra from GNASH runs, compute the recoil spectra, and format the results. Iron is being used as a test case because of its importance for the FMIT target design.

E. Steady-State Transfer Tables for Delayed Photons from Fission (R. J. LaBauve and D. C. George)

At the request of D. R. Harris, Chairman of the American Nuclear Society ANS 6.1.2 committee charged with producing the standard for preparing cross sections for shielding applications, we have produced steady-state transfer tables for delayed photons from fission in the BUGLE[19] multigroup structure. The photon energy bounds of the BUGLE set are given in Table III.

The scheme followed in producing these tables is that given in Ref. 20 where the delayed photon yield for a given photon group is given by the summation

$$y_g = \sum_{i=1}^{n} \frac{\alpha_{i,g}}{\lambda_{i,g}} \quad .$$

The $\alpha_{i,g}$ and $\lambda_{i,g}$ are obtained from fits to aggregate decay energy from a neutron pulse on a fissionable target as generated by CINDER and peripheral codes.[21] The FITPULS code[22] was used to obtain the fits in the BUGLE multigroup structure.

The steady-state tables were generated for the ten yield sets available in ENDF/B-IV, each yield set representing a particular fissioning target-incident neutron energy combination. The yield sets available in ENDF/B-IV are shown in Table IV. The data library used as input to FITPULS was the two-point-per-decade cooling time aggregate pulse data library described in Ref. 21. The tabulated steady-state results are given in Tables V through XIV. Note that the steady-state values are given in particles/fission as well as MeV/fission in these tables.

In order to investigate the validity of these results, several tests and comparisons were made. First, the steady-state results using the two-point-per decade data were compared with those from a six-point-per-decade fit. The aggregate fission product decay energy data in six-points-per-decade of cooling time were available only for the case of thermal neutrons incident on ^{235}U. For this comparison, groups 4 and 6 of the 11-group decay energy multigroup structure described in Ref. 21 were used since fits were already available. Group 4

TABLE III
BUGLE PHOTON GROUP STRUCTURE

Group No.	Lower (MeV)	E-Upper (MeV)
1	10.0	14.0
2	8.0	10.0
3	7.0	8.0
4	6.0	7.0
5	5.0	6.0
6	4.0	5.0
7	3.0	4.0
8	2.0	3.0
9	1.5	2.0
10	1.0	1.5
11	0.8	1.0
12	0.7	0.8
13	0.6	0.7
14	0.4	0.6
15	0.2	0.4
16	0.1	0.2
17	0.06	0.1
18	0.03	0.06
19	0.02	0.03
20	0.01	0.02

TABLE IV
FISSION DATA IN ENDF/B-IV

	Incident Neutron Energy Type		
Nuclide	Thermal	Fast	High Energy (14 MeV)
^{232}Th	--	Yes	No
^{233}U	Yes	No	No
^{235}U	Yes	Yes	Yes
^{238}U	--	Yes	Yes
^{239}Pu	Yes	Yes	No
^{241}Pu	Yes	No	No

TABLE V

STEADY STATE TABLE FOR TH-232 FAST

GROUP NO.	MEV/FIS	PAR/FIS
1	0.0000	0.0000
2	0.0000	0.0000
3	0.0000	0.0000
4	0.0087	0.0014
5	0.0719	0.0134
6	0.2437	0.0573
7	0.4169	0.1198
8	1.2324	0.5076
9	0.8651	0.5404
10	1.7531	1.3938
11	0.8997	1.0352
12	0.3782	0.5069
13	0.3957	0.6145
14	0.8767	1.7233
15	0.3667	1.2762
16	0.1468	1.0624
17	0.0684	0.8213
18	0.0090	0.1754
19	0.0007	0.0271
20	0.0002	0.0129

TABLE VI

STEADY STATE TABLE FOR U-233 THERMAL

GROUP NO.	MEV/FIS	PAR/FIS
1	0.0000	0.0000
2	0.0000	0.0000
3	0.0000	0.0000
4	0.0005	0.0030
5	0.0050	0.0269
6	0.0313	0.1333
7	0.0727	0.2519
8	0.2855	0.6850
9	0.3431	0.5384
10	0.8441	1.0555
11	0.6929	0.6077
12	0.4456	0.3344
13	0.4550	0.2964
14	0.9228	0.4691
15	0.8242	0.2386
16	0.5644	0.0816
17	0.2901	0.0239
18	0.1154	0.0055
19	0.0201	0.0005
20	0.0094	0.0001

TABLE VII

STEADY STATE TABLE FOR U-235 THERMAL

GROUP NO.	MEV/FIS	PAR/FIS
1	0.0000	0.0000
2	0.0000	0.0000
3	0.0000	0.0000
4	0.0045	0.0007
5	0.0366	0.0068
6	0.1608	0.0377
7	0.2924	0.0840
8	0.7976	0.3327
9	0.6234	0.3711
10	1.3115	1.0456
11	0.7824	0.8965
12	0.3933	0.5257
13	0.3513	0.5419
14	0.6698	1.3130
15	0.3183	1.0949
16	0.1121	0.7956
17	0.0438	0.5324
18	0.0079	0.1655
19	0.0005	0.0212
20	0.0002	0.0130

TABLE VIII

STEADY STATE TABLE FOR U-235 FAST

GROUP NO.	MEV/FIS	PAR/FIS
1	0.0000	0.0000
2	0.0000	0.0000
3	0.0000	0.0000
4	0.0045	0.0008
5	0.0361	0.0067
6	0.1546	0.0363
7	0.2808	0.0809
8	0.7813	0.3219
9	0.6150	0.3660
10	1.3063	1.0412
11	0.7873	0.8988
12	0.4045	0.5404
13	0.3540	0.5476
14	0.6724	1.3183
15	0.3259	1.1171
16	0.1131	0.8033
17	0.0446	0.5378
18	0.0082	0.1718
19	0.0005	0.0222
20	0.0002	0.0124

TABLE IX

STEADY STATE TABLE FOR U-235 HI-E

GROUP NO.	MEV/FIS	PAR/FIS
1	0.0000	0.0000
2	0.0000	0.0000
3	0.0000	0.0000
4	0.0045	0.0007
5	0.0332	0.0061
6	0.1306	0.0306
7	0.2567	0.0739
8	0.6265	0.2596
9	0.5425	0.3211
10	1.1093	0.8879
11	0.6886	0.7915
12	0.3577	0.4770
13	0.3237	0.4984
14	0.6215	1.2200
15	0.2889	0.9758
16	0.1019	0.7227
17	0.0420	0.5095
18	0.0077	0.1631
19	0.0005	0.0186
20	0.0002	0.0135

TABLE X

STEADY STATE TABLE FOR U-238 FAST

GROUP NO.	MEV/FIS	PAR/FIS
1	0.0000	0.0000
2	0.0000	0.0000
3	0.0000	0.0000
4	0.0082	0.0014
5	0.0545	0.0101
6	0.1785	0.0419
7	0.3241	0.0932
8	0.9209	0.3787
9	0.7228	0.4292
10	1.6242	1.2932
11	1.0838	1.2519
12	0.4119	0.5509
13	0.4410	0.6825
14	1.0424	2.0382
15	0.4497	1.5253
16	0.1706	1.2489
17	0.0882	1.0625
18	0.0124	0.2638
19	0.0006	0.0256
20	0.0002	0.0162

TABLE XI

STEADY STATE TABLE FOR U-238 HI-E

GROUP NO.	MEV/FIS	PAR/FIS
1	0.0000	0.0000
2	0.0000	0.0000
3	0.0000	0.0000
4	0.0067	0.0011
5	0.0452	0.0083
6	0.1524	0.0391
7	0.2782	0.0883
8	0.7680	0.3165
9	0.6180	0.3638
10	1.3881	1.1085
11	0.9661	1.1149
12	0.4109	0.5476
13	0.3990	0.6163
14	0.8904	1.7440
15	0.3928	1.3226
16	0.1514	1.0980
17	0.0737	0.8913
18	0.0104	0.2211
19	0.0005	0.0216
20	0.0002	0.0159

TABLE XII

STEADY STATE TABLE FOR PU-239 THERMAL

GROUP NO.	MEV/FIS	PAR/FIS
1	0.0000	0.0000
2	0.0000	0.0000
3	0.0000	0.0000
4	0.0028	0.0005
5	0.0209	0.0039
6	0.0959	0.0243
7	0.1956	0.0564
8	0.5680	0.2365
9	0.5015	0.2987
10	1.0018	0.7981
11	0.6329	0.7216
12	0.3404	0.4545
13	0.3349	0.5150
14	0.5638	1.1155
15	0.3121	1.0535
16	0.0904	0.6292
17	0.0315	0.3827
18	0.0092	0.2067
19	0.0005	0.0208
20	0.0002	0.0124

TABLE XIII

STEADY STATE TABLE FOR PU-239 FAST

GROUP NO.	MEV/FIS	PAR/FIS
1	0.0000	0.0000
2	0.0000	0.0000
3	0.0000	0.0000
4	0.0029	0.0005
5	0.0218	0.0041
6	0.1059	0.0231
7	0.2017	0.0582
8	0.5876	0.2445
9	0.5096	0.3033
10	1.0399	0.8298
11	0.6380	0.7279
12	0.3384	0.4515
13	0.3370	0.5186
14	0.5752	1.1408
15	0.3252	1.0963
16	0.0930	0.6438
17	0.0328	0.3993
18	0.0093	0.2078
19	0.0005	0.0207
20	0.0002	0.0128

TABLE XIV

STEADY STATE TABLE FOR PU-241 THERMAL

GROUP NO.	MEV/FIS	PAR/FIS
1	0.0000	0.0000
2	0.0000	0.0000
3	0.0000	0.0000
4	0.0046	0.0008
5	0.0319	0.0059
6	0.1338	0.0314
7	0.2412	0.0695
8	0.7065	0.2926
9	0.6030	0.3589
10	1.2474	0.9915
11	0.7846	0.8996
12	0.3409	0.4561
13	0.3814	0.5891
14	0.7402	1.4611
15	0.3887	1.3063
16	0.1207	0.8537
17	0.0521	0.6311
18	0.0108	0.2344
19	0.0006	0.0242
20	0.0002	0.0148

is the energy bin from 1.35 to 1.8 MeV and group 6 is the bin from 2.2 to 2.6 MeV. Figures 10 and 11, respectively, show the fits for groups 4 and 6 using the six-point-per-decade data and Figs. 12 and 13 the fits for the two-point-per-decade data. Note that the slope reversal in group 6 near 10^5 s cooling time evident for the six-point-per-decade data is not seen in the two-point-per-decade data.

Steady-state results were quite similar for the two sets of data. For group 4, a value of 0.971 MeV/fis was obtained from the two-point-per-decade data that is to be compared with 1.012 MeV/fis obtained from the six-point-per-decade data. For group 6, the values are 0.410 MeV/fis and 0.423 MeV/fis, respectively. As the differences of 3% for group 4 and 5% for group 6 are relatively smaller than differences arising from other considerations described below, we conclude that the two-point-per-decade data are adequate for this application.

As a second test of the validity of these results, comparisons of our steady-state values were made with those from ORNL.[23] These are shown in Figs. 14 through 18. The differences seen in the figures arise mainly from the methods of dealing with "missing" spectra in ENDF/B-IV. The ENDF/B-IV library contains complete evaluations, including spectra, for only 181 fission products of the 711 unstable nuclides needed for the summation codes CINDER (LASL) and ORIGEN (ORNL). The scheme we have used for "constructing" a missing spectrum for a particular nuclide is described in Ref. 18 and consists of spreading out the average decay energy given for the nuclide over a spectral shape derived from the aggregate decay energy of 181 nuclides from a pulse after a cooling time approximately equal to the half-life of the nuclide in question. In the ORNL scheme, the "shape" of the missing spectrum is assumed to be a single line located at the average decay energy; it is thus understandable that the ORNL steady-state results seem to be "harder" than ours. The ORNL results also include an estimate of the contribution of x rays to the lower energy groups. X-ray data is essentially absent in ENDF/B-IV.

In the last comparison made, photon data from the Julich GAMDAT78 library[24] were used to replace that in ENDF/B-IV wherever possible. For consistency, however, the spectrum of each nuclide taken from the GAMDAT78 file was normalized to the average total photon energy of this nuclide given by the ENDF/B-IV file. Of the 711 original nuclides, 302 were replaced with data from GAMDAT78; of

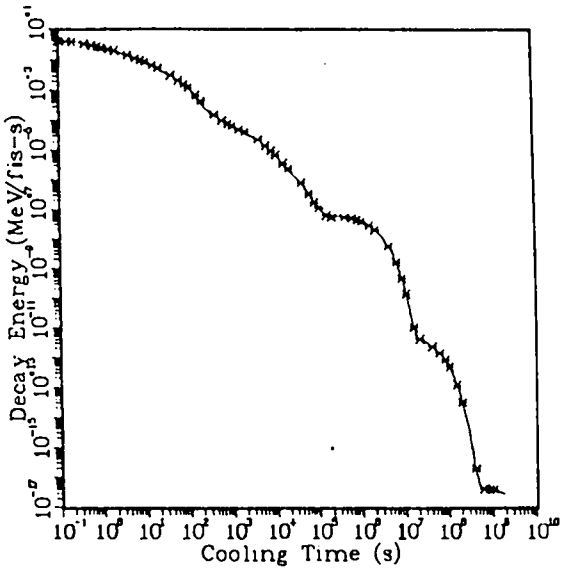

Fig. 10.
Gamma fit, group 4 (6 points/ decade).

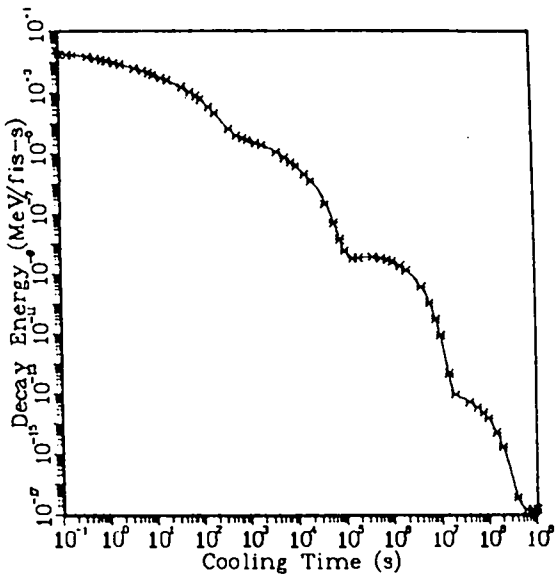

Fig. 11.
Gamma fit, group 6 (6 points/ decade).

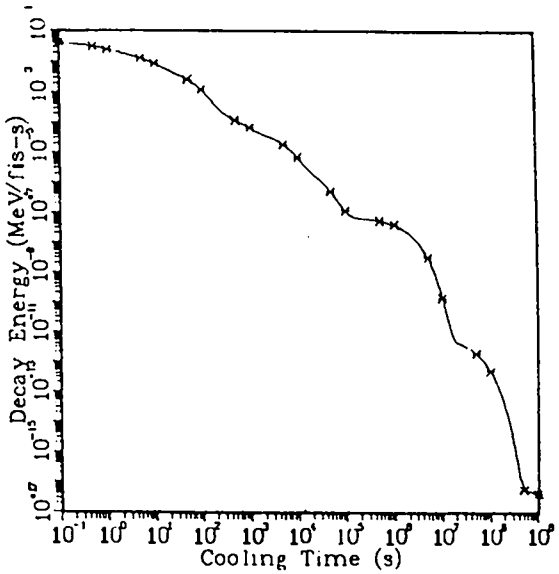

Fig. 12.
Gamma fit, group 4 (2 points/ decade).

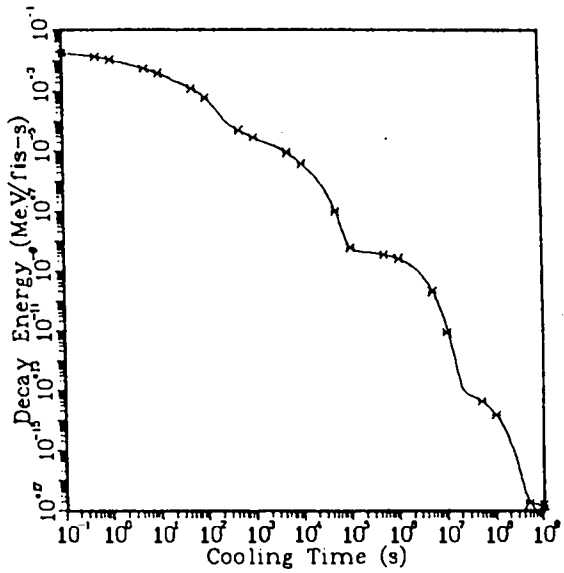

Fig. 13.
Gamma fit, group 6 (2 points/ decade).

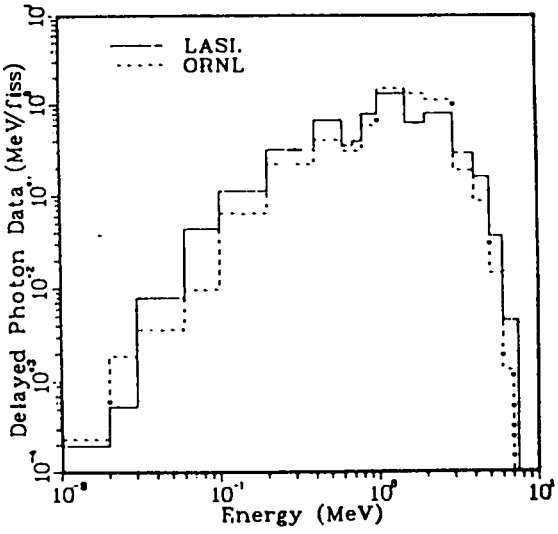

Fig. 14.
Comparison of LASL and ORNL steady-state values for ^{235}U thermal fission.

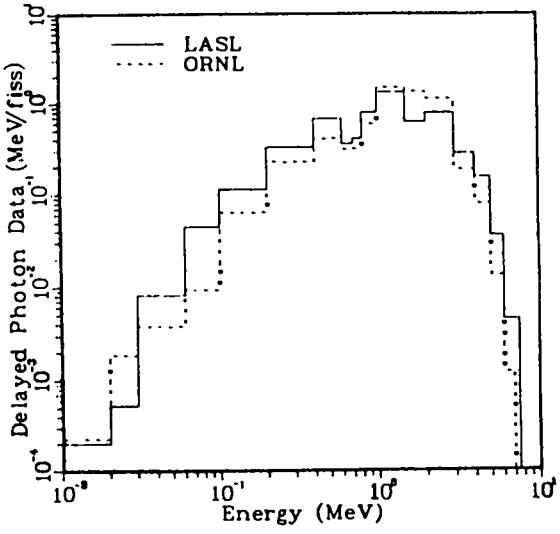

Fig. 15.
Comparison of LASL and ORNL steady-state values for ^{235}U fast fission.

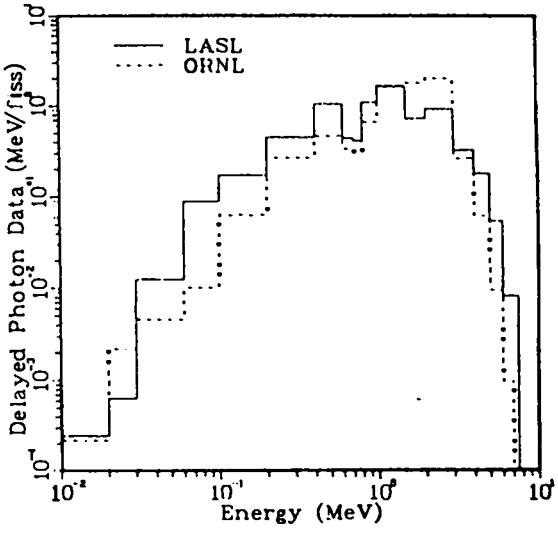

Fig. 16.
Comparison of LASL and ORNL steady-state values for ^{238}U fast fission.

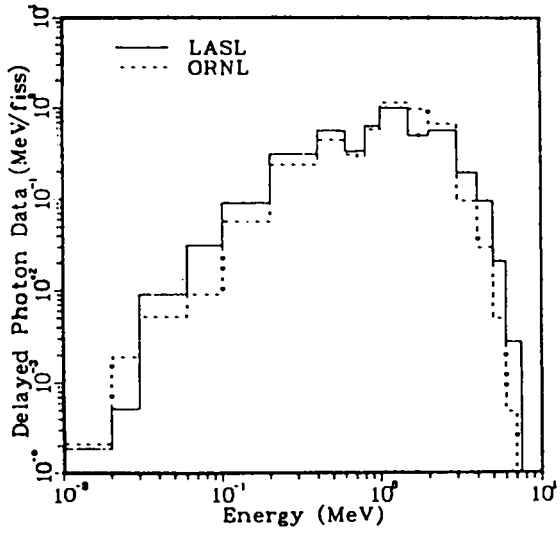

Fig. 17.
Comparison of LASL and ORNL steady-state values for ^{239}Pu thermal fission.

these, 144 with "constructed" spectra were replaced. Only 14 of the nuclides with spectra in ENDF/B-IV were not replaced with data from GAMDAT78.

Results are compared in Fig. 19. Note that the comparison is fair to good for all but the low-energy groups. Here the GAMDAT78 results are generally higher than those from ENDF/B-IV due to the fact that the GAMDAT78 library includes x-ray data. There is also a rather large, unaccounted for discrepancy in group 16; however, large differences do occur in the spectra of individual nuclides, and these may be responsible for this effect.

In conclusion, we feel that although this study has produced a useful set of steady-state tables of delayed photon data, greater accuracy would be achieved with a better basic data library containing more nuclides with spectra. In particular, the ENDF/B-V fission-product file that is now being tested by LASL and other members of CSEWG will contain some 261 nuclides with gamma and/or x-ray spectral data. This file should be compared and augmented with data from other existing files such as GAMDAT78.

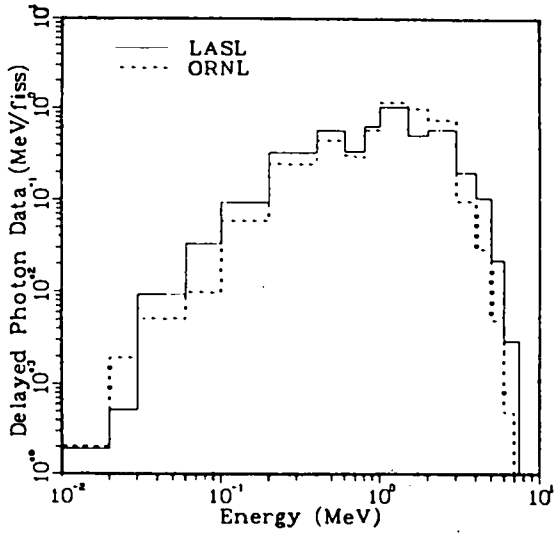

Fig. 18.
Comparison of LASL and ORNL steady-state values for ^{239}Pu fast fission.

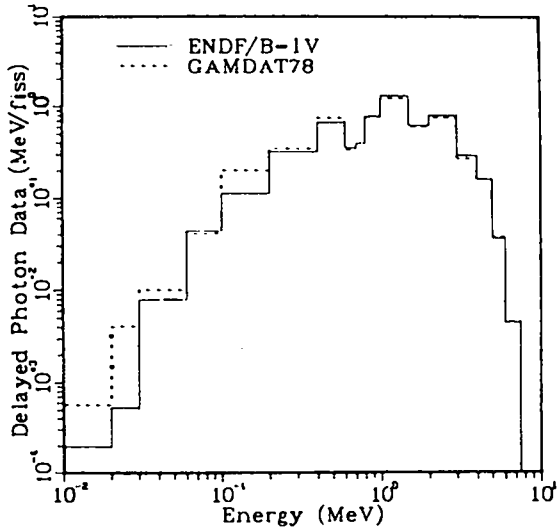

Fig. 19.
Comparison of ENDF/B-IV data with GAMDAT78 data for ^{235}U thermal fission.

III. FISSION PRODUCTS AND ACTINIDES: YIELDS, DECAY DATA, DEPLETION, AND BUILDUP

A. ENDF/B-V Spectral Code (T. R. England and N. L. Whittemore)

This code is being developed as a general processing code for the new ENDF/B-V extended decay files. Capabilities to generate the following data have been completed and tested.

- Multigroup and total gamma and x-ray energies and multiplicities.
- Multigroup and total beta, positron, and neutrino energies and particle distributions.

The beta (positron) routine includes correction factors for first, second, and third forbidden unique distributions and for external screening electrons. The relativistic form of the Fermi distribution function F(Z,W) is used.

The routine also incorporates a special compact print of all major decay parameters similar to the ENDF/B-IV tables in LASL report LA-6116-MS. To date, the routine has been applied to the preliminary fission product files, all activation nuclides, and 60 actinides in ENDF/B-V. Modules for gamma-line broadening, alpha spectra, and discrete electron spectra have yet to be added.

B. Summary of Actinide Decay Data in ENDF/B-V (T. R. England, W. B. Wilson, and N. L. Whittemore)

A summary of the ENDF/B-V actinide decay parameters is given in Table XV for 60 actinides. Average decay energies and Q-values are listed in units of eV, half-lives in units of seconds. RTYP denotes the principle mode of decay where:

RTYP	Decay Mode
1.0	β^-
2.0	β^+ and/or e.c.
3.0	γ
4.0	α
5.0	n (neutrons other than delayed)
6.0	spontaneous fission
7.0	p
10.0	unknown origin

Combined values such as 1.5 refer to beta followed by neutron emission. NDK is the number of decay modes and NSP the number of spectral types for each nuclide.

Data for the 60 actinides in Table XV show that all are unstable, 3 are in first isomeric states (none are in second isomeric states), all have spectral data, 22 have beta spectra, 57 have gamma spectra, 42 have alpha spectra, 8 have positron and/or e.c. spectra, 56 have x-ray spectra, 54 have conversion electron coefficients, and 23 have spontaneous fission branching fractions.

Also, comparisons with spectral calculations show errors in ^{232}Th, ^{244}Pu, ^{248}Cm, and ^{253}Cf. These will be corrected in future ENDF/B-V MODS.

C. Fission Product Testing for ENDF/B-V (T. R. England and N. L. Whittemore)

The physics checking code noted in the last progress report continues to be used in tests of the ENDF/B-V files (Phase 1 review). The results have been supplied to the chairman of the ENDF/B Fission Product and Actinide Subcommittee of CSEWG. The files are not yet complete and still contain some inconsistent data.

The basic content of the files represents an enormous expansion over ENDF/B-IV, particularly in spectra and fission yields. A comparison is given in Table XVI.

D. Neutrino Spectra (T. R. England and N. L. Whittemore)

The proposed P-14 neutrino (actually antineutrino) experiment (H. Kruse, R. Loncoski) includes a request for T-2 calculations of the aggregate neutrino spectra. This requires temporal concentrations of fission products using, e.g., the CINDER code folded with the decay constants of each nuclide and their corresponding neutrino spectra. The spectra above the approximately 1.8 MeV threshold for the inverse β^- decay reaction $\bar{\nu} + p \rightarrow n + \beta^+$ is of primary interest.

The spectral code described in Sec. III.A of this report will be used to produce the neutrino spectra per nuclide using augmented ENDF/B-V data. The module has been tested using a preliminary ENDF/B-V file. Figure 20 shows a plot of β^- spectra and corresponding neutrino spectra for a single beta endpoint energy of 7.2 MeV (Z = 50). Figure 21 shows the β^- and neutrino spectra for ^{80}As. This nuclide has 13 beta endpoints (the dominant values occur at 3.69, 4.04, 4.13, 5.33, and 6.00 MeV, with the last two points being most dominant). There were 158 energy groups used in these calculations; a correction for external electron screening is included.

TABLE XV

SUMMARY OF DECAY PARAMETERS FOR 60 ENDF/B-V ACTINIDES

NO	SYMBOL	S	ZZAAAS	HALFLIFE	E-BETA	E-GAMMA	E-ALPHA	RTYP	RFS	Q	BRANCHING	NDK	NSP	MAT
1	81-TL-208	0	812080	1.[illegible]E+02	5.8920E+05	3.3910E+06	0.	1.00	0.0	4.9920E+06	1.0000E+00	1	4	8108
2	82-PB-212	0	822120	3.[illegible]E+04	1.7200E+05	1.4500E+05	0.	1.00	0.0	5.7280E+05	1.0000E+00	1	4	8212
3	83-BI-212	0	832120	3.[illegible]E+03	5.0300E+05	1.0570E+05	7.9550E+06	1.00	0.0	2.2460E+06	0.	3	5	8312
								4.00	0.0	6.2074E+06	3.5930E-01			
								1.40	0.0	1.1200E+07	6.4070E-01			
4	84-PO-216	0	842160	1.5000E-01	0.	1.7000E+01	6.9064E+06	4.00	0.0	6.9066E+06	1.0000E+00	1	2	8416
5	86-RN-220	0	862200	5.5600E+01	0.	5.0000E+02	6.4043E+06	4.00	0.0	6.4049E+06	1.0000E+00	1	2	8620
6	88-RA-224	0	882240	3.1622E+05	2.3000E+03	1.0000E+04	5.7780E+06	4.00	0.0	5.7890E+06	1.0000E+00	1	4	8824
7	90-TH-228	0	902280	6.0372E+07	1.9100E+04	3.5100E+03	5.4960E+06	4.00	0.0	5.5203E+06	1.0000E+00	1	4	8028
8	90-TH-230	0	902300	2.6200E+12	1.2490E+04	1.3980E+03	4.7470E+06	4.00	0.0	4.7706E+06	1.0000E+00	1	4	8030
9	90-TH-231	0	902310	9.1972E+04	1.2880E+05	2.4900E+04	0.	1.00	0.0	3.9000E+05	1.0000E+00	1	4	8031
10	91-PA-231	0	912310	1.0138E+12	1.6650E+04	3.2400E+04	5.0110E+06	4.00	0.0	5.1484E+06	1.0000E+00	1	4	8131
11	90-TH-232	0	902320	4.4337E+17	1.1100E+04	1.1000E+03	4.0760E+06	4.00	0.0	4.0820E+06	1.0000E+00	1	2	1390
12	91-PA-232	0	912320	1.1318E+05	1.5800E+05	9.4000E+05	0.	1.00	0.0	1.3370E+06	1.0000E+00	1	4	8132
13	92- U-232	0	922320	2.2426E+09	1.2740E+04	2.2179E+05	5.3996E+06	4.00	0.0	5.4139E+06	1.0000E+00	2	4	8232
								6.00	0.0	0.	9.0000E-13			
14	90-TH-233	0	902330	1.3380E+05	4.0690E+05	9.5347E+04	0.	1.00	0.0	1.2452E+06	1.0000E+00	1	4	8033
15	91-PA-233	0	912330	2.3328E+06	1.8900E+05	2.1900E+05	0.	1.00	0.0	5.7230E+05	1.0000E+00	1	4	1391
16	92- U-233	0	922330	5.0232E+12	3.7400E+03	1.0700E+03	4.8930E+06	4.00	0.0	4.9091E+06	1.0000E+00	2	4	1393
								6.00	0.0	0.	1.3000E-12			
17	92- U-234	0	922340	7.7188E+12	1.0900E+04	1.6100E+03	4.8560E+06	4.00	0.0	4.8564E+06	1.0000E+00	2	4	1394
								6.00	0.0	0.	1.2000E-11			
18	92- U-235	0	922350	2.2210E+16	2.4100E+04	1.7000E+03	4.4710E+06	4.00	0.0	4.6790E+06	1.0000E+00	1	4	1395
19	92- U-236	0	922360	7.3990E+14	9.2000E+03	1.6700E+03	4.5700E+06	4.00	0.0	4.5692E+06	1.0000E+00	2	4	1396
								6.00	0.0	0.	1.2000E-09			
20	93-NP-236	1	932361	8.1000E+04	8.3400E+04	5.1900E+04	0.	1.00	0.0	5.3700E+05	4.8000E-01	2	5	8346
								2.00	0.0	9.8500E+05	5.2000E-01			
21	93-NP-236	0	932360	3.6290E+12	1.8700E+05	1.5200E+05	0.	1.00	0.0	5.3700E+05	8.9000E-02	2	5	8336
								2.00	0.0	9.8500E+05	9.1100E-01			
22	94-PU-236	0	942360	8.9969E+07	1.0120E+04	2.2300E+03	5.8510E+06	4.00	0.0	5.8677E+06	1.0000E+00	2	4	8436
								6.00	0.0	0.	8.1000E-10			
23	92- U-237	0	922370	6.7830E+05	1.6730E+05	1.4300E+05	0.	1.00	0.0	5.1910E+05	1.0000E+00	1	4	8237
24	93-NP-237	0	932370	6.7532E+13	4.7000E+04	3.9000E+04	4.8650E+06	4.00	0.0	4.9573E+06	1.0000E+00	1	4	1337
25	94-PU-237	0	942370	3.9424E+06	6.1200E+03	5.6500E+04	1.8000E+02	2.00	0.0	2.2400E+05	1.0000E+00	2	5	8437
								4.00	0.0	5.7540E+06	3.3000E-05			
***BRANCHINGS DO NOT SUM TO 1.0. VALUE=1.000033E+00														
26	92- U-238	0	922380	1.4100E+17	9.1000E+03	1.4000E+03	4.2660E+06	4.00	0.0	4.2710E+06	1.0000E+00	2	4	1398
								6.00	0.0	0.	5.4500E-07			
27	93-NP-238	0	932380	1.8291E+05	2.4960E+05	5.4800E+05	0.	1.00	0.0	1.2930E+06	1.0000E+00	1	4	8338
28	94-PU-238	0	942380	2.7691E+09	8.2600E+03	1.8620E+03	5.5770E+06	4.00	0.0	5.5933E+06	1.0000E+00	2	4	1338
								6.00	0.0	0.	1.8400E-09			
29	92- U-239	0	922390	1.4100E+03	4.1100E+05	5.4000E+04	0.	1.00	0.0	1.2670E+06	1.0000E+00	1	4	8239
30	93-NP-239	0	932390	2.0333E+05	2.4300E+05	1.7500E+05	0.	1.00	0.0	7.2140E+05	1.0000E+00	1	4	8339
31	94-PU-239	0	942390	7.6034E+11	3.8300E+03	8.1400E+02	5.2350E+06	4.00	0.0	5.2435E+06	1.0000E+00	2	4	1399
								6.00	0.0	0.	4.4000E-12			
32	94-PU-240	0	942400	2.0670E+11	9.2800E+03	1.6470E+03	5.2430E+06	4.00	0.0	5.2560E+06	1.0000E+00	2	4	1380
								6.00	0.0	0.	5.0000E-08			
33	95-AM-240	0	952400	1.9288E+05	5.7000E+04	1.0350E+06	1.0380E+01	2.00	0.0	1.3460E+06	1.0000E+00	2	5	8540
								4.00	0.0	5.7000E+06	1.9000E-06			
***BRANCHINGS DO NOT SUM TO 1.0. VALUE=1.000002E+00														
34	94-PU-241	0	942410	4.8399E+08	5.2400E+03	4.1700E-01	1.2200E+02	1.00	0.0	2.0820E+04	1.0000E+00	2	3	1381
								4.00	0.0	5.1396E+06	2.4500E-05			

TABLE XV (cont)

***BRANCHINGS DO NOT SUM TO 1.0, VALUE=1.000024E+00													
35	95-AM-241	0	952410	1.3439E+10	1.7500E+04	2.8600E+04	5.5670E+06	4.00	0.0	5.6379E+06	1.0000E+00	2	4 1361
								6.00	0.0	0.	4.1000E-12		
36	96-CM-241	0	962410	2.8339E+05	5.3700E+05	5.1700E+05	6.0000E+04	2.00	0.0	7.7100E+05	9.9000E-01	2	5 8641
								4.00	0.0	6.1848E+06	1.0000E-02		
37	94-PU-242	0	942420	1.1975E+13	6.7700E+03	1.4000E+03	4.9730E+06	4.00	0.0	4.9831E+06	1.0000E+00	2	4 1342
								6.00	0.0	0.	5.5000E-06		
***BRANCHINGS DO NOT SUM TO 1.0, VALUE=1.000005E+00													
38	95-AM-242	1	952421	4.7966E+09	3.2200E+04	5.9000E+03	2.5000E+04	3.00	0.0	4.8630E+04	9.9500E-01	3	4 1369
								4.00	0.0	5.6380E+06	4.7600E-03		
								6.00	0.0	0.	1.6000E-10		
***BRANCHINGS DO NOT SUM TO 1.0, VALUE=9.997600E-01													
39	95-AM-242	0	952420	5.7436E+04	1.7510E+05	1.9310E+04	0.	1.00	0.0	6.6500E+05	8.2700E-01	2	5 8542
								2.00	0.0	7.9200E+05	1.7300E-01		
40	96-CM-242	0	962420	1.4074E+07	7.7000E+03	2.2000E+03	6.2070E+06	4.00	0.0	6.2158E+06	1.0000E+00	2	4 8642
								6.00	0.0	0.	6.8000E-08		
41	94-PU-243	0	942430	1.7445E+04	1.7070E+05	2.9000E+04	0.	1.00	0.0	5.8300E+05	1.0000E+00	1	4 8443
42	95-AM-243	0	952430	2.3289E+11	1.4200E+04	6.0000E+04	5.3482E+06	4.00	0.0	5.4387E+06	1.0000E+00	2	4 1363
								6.00	0.0	0.	2.2000E-10		
43	96-CM-243	0	962430	8.9937E+08	1.0260E+05	1.2780E+05	5.9294E+06	2.00	0.0	7.2000E+03	2.6000E-03	2	5 1343
								4.00	0.0	6.1674E+06	9.9740E-01		
44	94-PU-244	0	942440	2.5977E+15	0.	0.	4.6510E+06	4.00	0.0	4.6658E+06	9.9875E-01	2	3 8444
								6.00	0.0	0.	1.2500E-03		
45	95-AM-244	1	952441	1.5600F+03	5.0700E+05	1.8300E+03	0.	1.00	0.0	1.4980E+06	9.9961E-01	2	5 8554
								2.00	0.0	1.4000E+05	3.9000E-04		
46	95-AM-244	0	952440	3.6350E+04	3.1000E+05	8.0770E+05	0.	1.00	0.0	1.4290E+06	1.0000E+00	1	4 8544
47	96-CM-244	0	962440	9.7149E+09	6.4000E+03	1.6050E+03	5.8930E+06	4.00	0.0	5.9018E+06	1.0000E+00	2	4 1344
								6.00	0.0	0.	1.3470E-06		
***BRANCHINGS DO NOT SUM TO 1.0, VALUE=1.000001E+00													
48	96-CM-245	0	962450	2.6744E+11	4.0800E+04	1.0200E+05	5.4453E+06	4.00	0.0	5.6235E+06	1.0000E+00	1	4 1345
49	96-CM-246	0	962460	1.4926E+11	5.9800E+03	1.3760E+03	5.4640E+06	4.00	0.0	5.4760E+06	9.9974E-01	2	4 1346
								6.00	0.0	0.	2.6140E-04		
50	96-CM-247	0	962470	4.9229E+14	1.0200E+04	3.1400E+05	5.0280E+06	4.00	0.0	5.3530E+06	1.0000E+00	1	4 8647
51	96-CM-248	0	962480	1.0720F+13	0.	0.	4.7270E+06	4.00	0.0	5.1610E+06	9.1740E-01	2	3 8648
								6.00	0.0	0.	8.2600E-02		
52	96-CM-249	0	962490	3.8490F+03	2.7400E+05	1.9200E+04	0.	1.00	0.0	9.0300E+05	1.0000E+00	1	4 8649
53	97-BK-249	0	972490	2.7648E+07	3.3000E+04	8.8000E-02	7.9000E+01	1.00	0.0	1.2640E+05	9.9998E-01	3	5 8749
								4.00	0.0	5.5260E+06	1.4500E-05		
								6.00	0.0	0.	4.6000E-10		
54	98-CF-249	0	982490	1.1064E+10	1.8300E+04	3.2800E+05	5.9440E+06	4.00	0.0	6.2956E+06	1.0000E+00	2	4 8849
								6.00	0.0	0.	5.0200E-09		
55	97-BK-250	0	972500	1.1581E+04	2.8390E+05	8.9900E+05	0.	1.00	0.0	1.7750E+06	1.0000E+00	1	4 8750
56	98-CF-250	0	982500	4.1276E+09	4.2500E+03	1.4600E+03	6.1170E+06	4.00	0.0	6.1292E+06	9.9923E-01	2	4 8850
								6.00	0.0	0.	7.7000E-04		
57	98-CF-251	0	982510	2.8338E+10	1.2900E+05	1.0600E+05	5.7910E+06	4.00	0.0	6.1724E+06	1.0000E+00	1	4 8851
58	98-CF-252	0	982520	8.3247E+07	4.1700E+03	1.4800E+03	6.0260E+06	4.00	0.0	6.2171E+06	9.6908E-01	2	4 8852
								6.00	0.0	0.	3.0920E-02		
59	98-CF-253	0	982530	1.5388F+05	7.9000E+04	0.	1.9000E+04	1.00	0.0	2.8900E+05	9.9690E-01	2	3 8853
								4.00	0.0	6.1260E+06	3.1000E-03		
60	99-ES-253	0	992530	1.7696E+04	2.3700E+03	1.3720E+03	6.7330E+06	4.00	0.0	6.7396E+06	1.0000E+00	2	4 8953
								6.00	0.0	0.	8.7000E-08		

TABLE XVI

ENDF/B-IV vs ENDF/B-V
GROSS COMPARISON OF DATA CONTENT IN FP FILES

TYPE OF QUANTITY	ENDF/B-IV	ENDF/B-V
General Content		
Total nuclides	824	877
Nuclides having cross sections	181	196
Stable nuclides	113	127
Unstable nuclides	711	750
Total isomeric states (0.1s)	123	154
First isomeric states (0.1s)	117	148
Average energies derived from exp.	181	317
Delayed neutron precursors	57	105
Fission yield sets	10	20
Nuclides having detailed spectral data		
Beta and/or gamma	180	264
Electron related	163 (β^- only)	233
Photon related	172 (γ only)	247
Conversion electron	38	157
Positron or EC	0	12
X Ray	0	166
Discrete electron	0	166

Fission yield data: 10 sets of direct yields in ENDF/B-IV ($\sim$ 11 000 yields).

20 sets of direct and cumulative (by A and Z) yields in ENDF/B-V, now including uncertainties ($\sim$ 44 000 yields plus uncertainties).

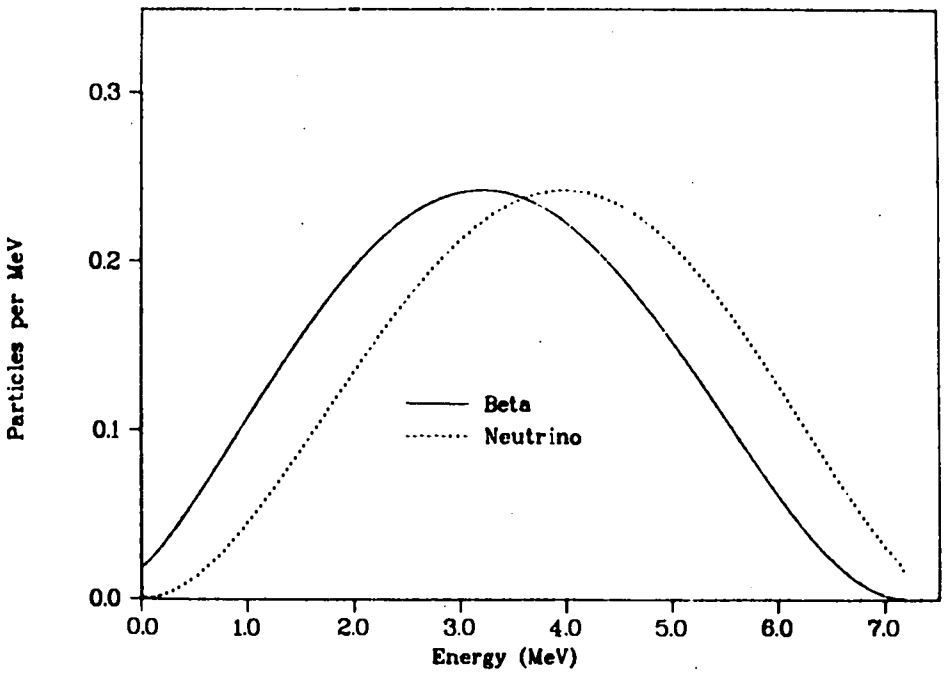

Fig. 20.
Beta and neutrino spectra for 7.2 MeV endpoint energy.

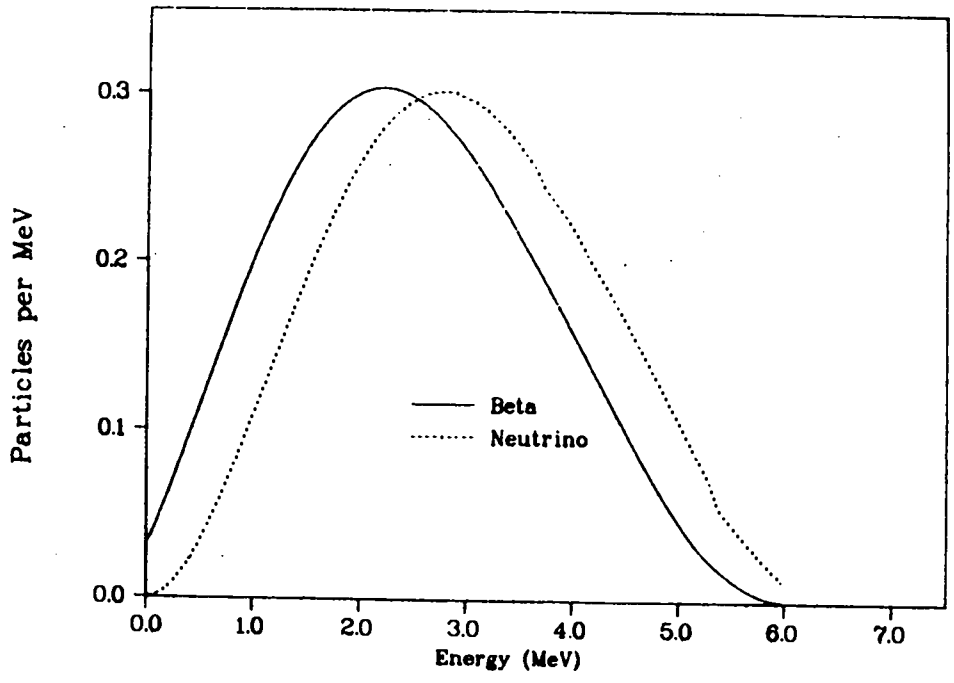

Fig. 21
Beta and neutrino spectra for ^{80}As.

Augmentation of the ENDF/B-V data will be necessary because only approximately 261 of the 750 unstable fission products have evaluated spectra. These 261, however, are the most important contributors because of their relatively large fission yields. Some unstable nuclides have no measured spectra and a spectral model based on Q-values will be necessary for these. Most are not important contributors to the beta and neutrino spectra.

E. CINDER Actinide Decay Library Development (W. B. Wilson, T. R. England, R. J. LaBauve, M. Battat, and N. L. Whittemore)

A total of 144 heavy element nuclides ranging from $^{206}_{80}Hg$ to $^{258}_{100}Fm$ have been identifed from available nuclear data sources as actinide products in reactor fuel. The decay modes of these nuclei include β^-, β^+, electron capture, internal conversion, and isomeric transition (in which A is unchanged), as well as alpha decay (in which A decreases by 4), and spontaneous fission. As a result, the group of nuclides can be separated into four unique sets with stable end products $^{206}_{82}Pb$, $^{207}_{82}Pb$, $^{208}_{82}Pb$, or $^{209}_{83}Bi$. These nuclide sets are identified in Figs. 22-25, respectively.

Data for 60 of the nuclei are available from ENDF/B-V, as noted in Sec. III.B. Data of preliminary Canadian[25] and British[26] actinide evaluations have been supplied to us for evaluation and comparison. Additional information has been obtained from the recent editions of the Chart of the Nuclides[27] and Table of Isotopes.[28]

A program EBARDK has been written to calculate average alpha, beta, and gamma decay energy from decay scheme data. A library of decay data, including Q-values, transition probabilities, and energy levels for each transition has been partially completed with information extracted from Ref. 28. Parent and daughter spin and parity values are used to identify allowed and forbidden unique transitions. Average β^- or β^+ energies are determined using the method of Ref. 29. Average alpha and gamma decay energies are calculated from decay scheme energetics.

The gamma energies and intensities of Ref. 28 are also recorded in the library for future spectra library calculations. Beta spectra will also be calculated using the ENDF/B-V spectral code described above.

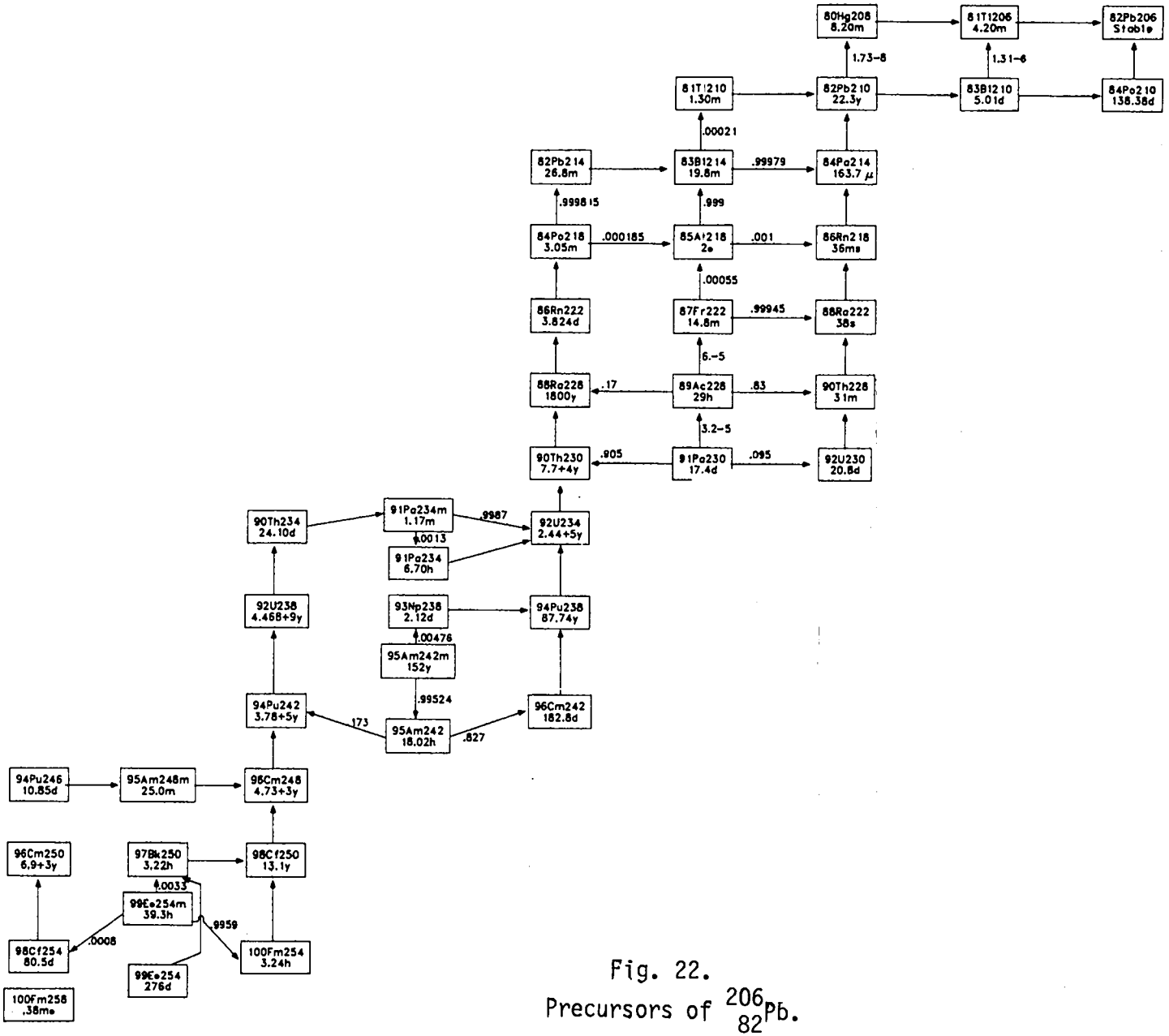

Fig. 22.
Precursors of $^{206}_{82}Pb$.

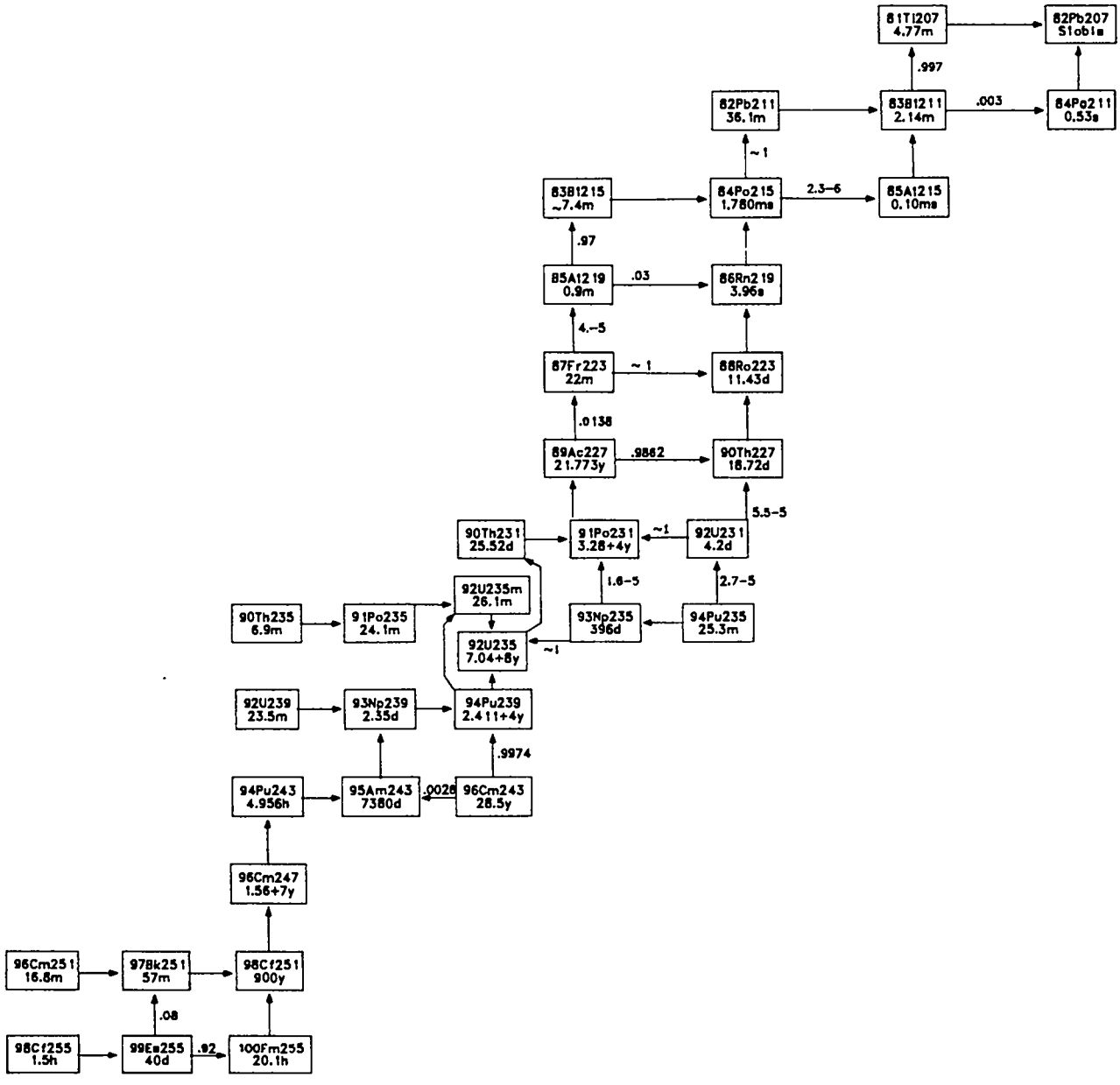

Fig. 23.

Precursors of $^{207}_{82}Pb$.

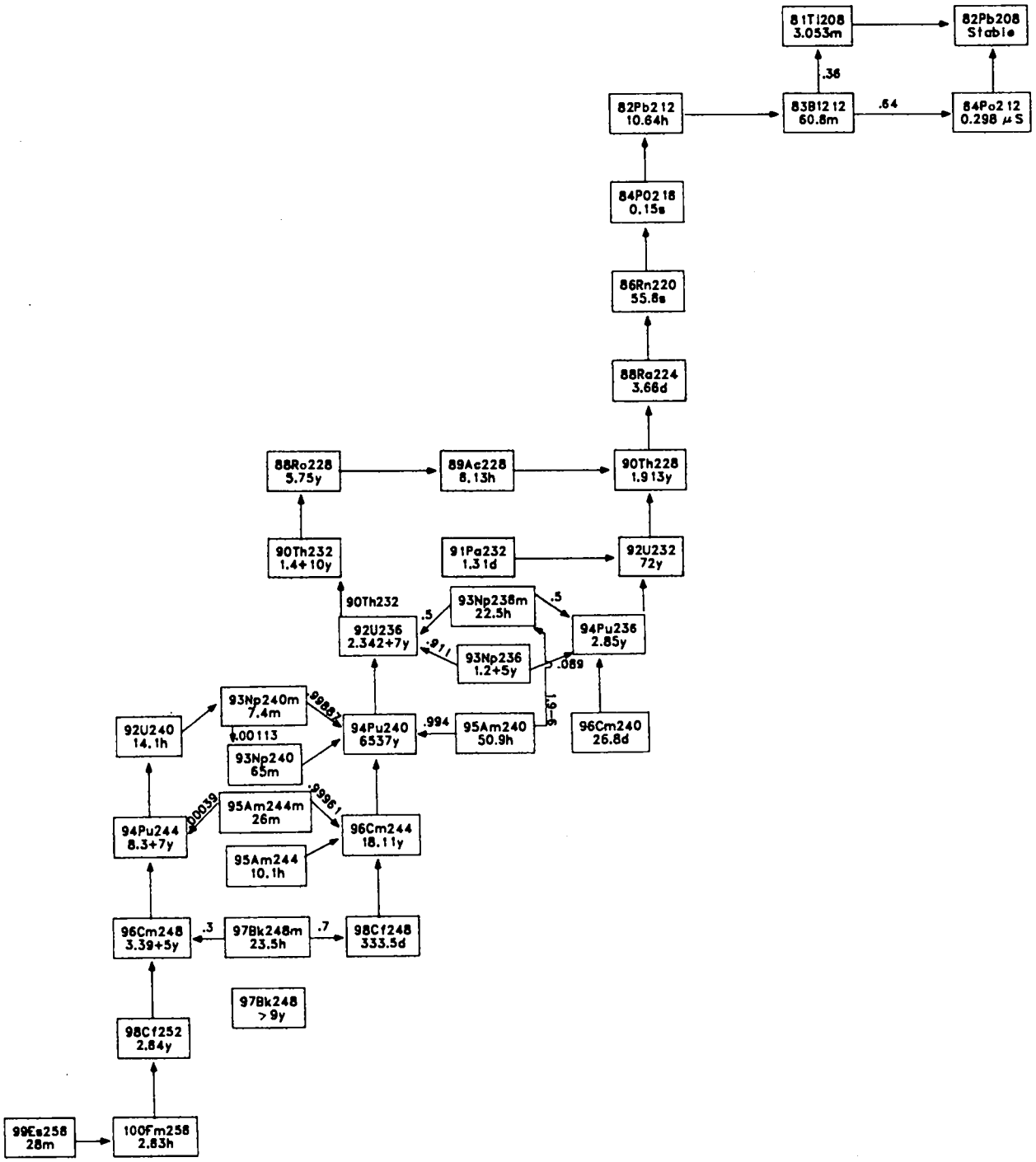

Fig. 24.
Precursors of $^{208}_{82}Pb$.

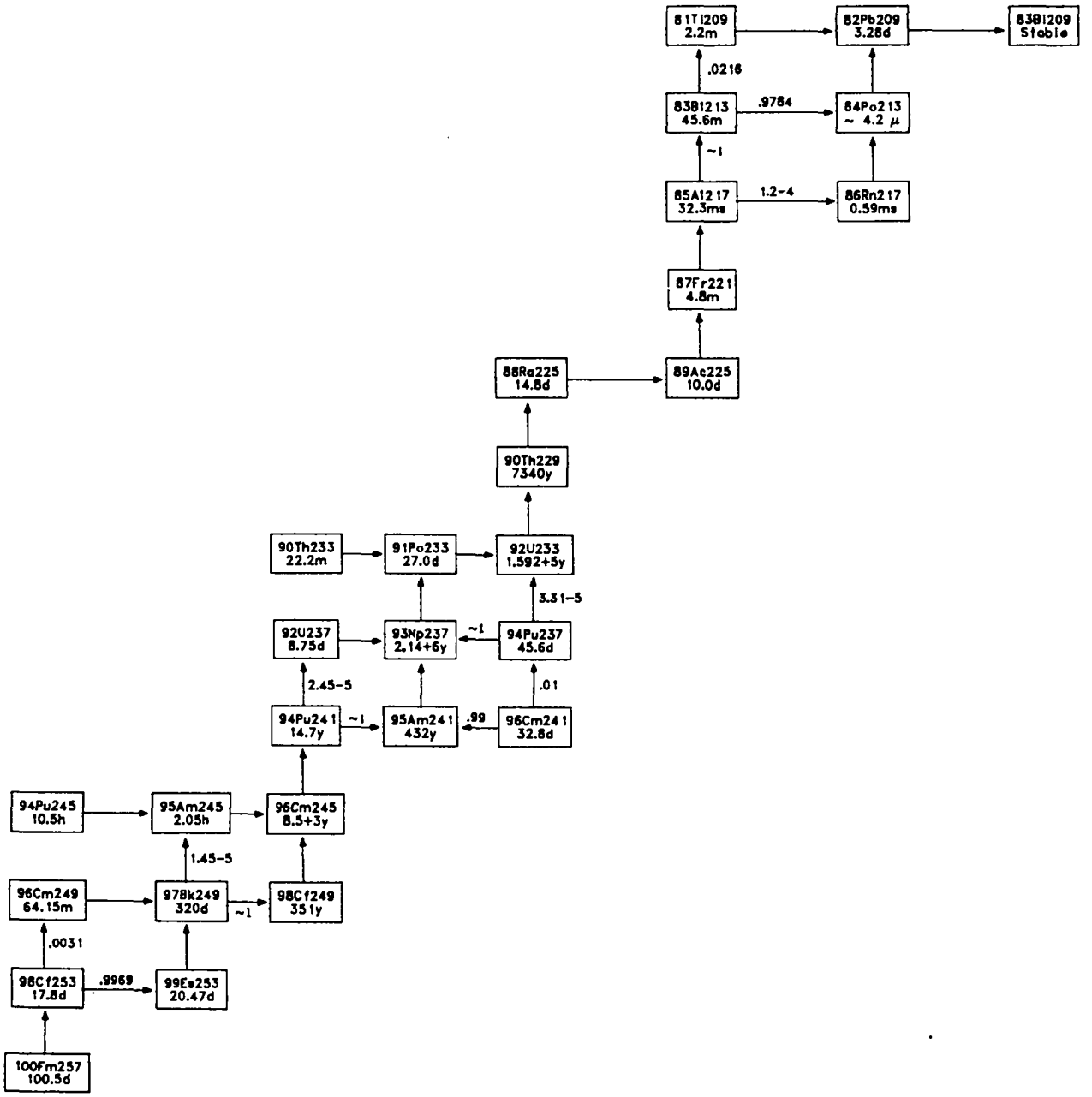

Fig. 25.
Precursors of $^{209}_{83}Bi$.

REFERENCES

1. J. J. Devaney and M. L. Stein, "Plasma Energy Deposition from Nuclear Elastic Scattering," Nucl. Sci. Eng. 46, 323 (1971).

2. S. T. Perkins and D. E. Cullen, "Elastic Nuclear (Plus Interference) Cross Sections for Light Nuclei," submitted to Nucl. Sci. Eng. (1980).

3. E. D. Arthur, "Calculation of Neutron Cross Sections on Isotopes of Yttrium and Zirconium," Los Alamos Scientific Laboratory report LA-7789-MS (1979).

4. R. J. Howerton, personal communication of ENDL-78; see also R. J. Howerton, D. E. Cullen, R. C. Haight, M. H. MacGregor, S. T. Perkins, and E. F. Plechatt, "The LLL Evaluated Nuclear Data Library (ENDL): Evaluation Techniques, Reaction Index, and Description of Individual Evaluations," Lawrence Livermore Laboratory report UCRL-50400 Vol. 15, Part A (Sept. 1975).

5. M. Walt, R. L. Becker, A. Okazaki, and R. E. Fields, "Total Fast Neutron Cross Sections of Co, Ga, Se, Cd, Te, Pt, Au, Hg, and Th," Phys. Rev. 89, 1271 (1953).

6. D. G. Foster, Jr., and D. W. Glasgow, "Neutron Total Cross Sections, 2.5-15 MeV, Part 1 Experimental," Phys. Rev. C3, 576 (1971).

7. J. Frehaut and G. Mosinski, "Measurement of (n,2n) and (n,3n) Cross Sections at Incident Energies Between 8 and 15 MeV," Proc. Conf. on Neutron Physics, Kiev (1975).

8. D. I. Garber and R. R. Kinsey, "Neutron Cross Sections Volume II, Curves," Brookhaven National Laboratory report BNL-325 (1976).

9. David G. Madland and J. Rayford Nix, "Calculation of Neutron Spectra and Average Neutron Multiplicities from Fission," submitted for presentation at the Int. Conf. on Nuclear Physics, Berkeley, CA (Aug. 24-30, 1980).

10. D. G. Madland and J. R. Nix, "Calculation of Prompt Fission Neutron Spectra," to be published.

11. P. I. Johansson and B. Holmqvist, "An Experimental Study of the Prompt Fission Neutron Spectrum Induced by 0.5-MeV Neutrons Incident on Uranium-235," Nucl. Sci. Eng. 62, 695 (1977).

12. F. D. Becchetti, Jr., and G. W. Greenlees, "Nucleon-Nucleus Optical-Model Parameters, $A < 40$, $E > 50$ MeV," Phys. Rev. 182, 1190 (1969).

13. B. L. Berman, "Atlas of Photoneutron Cross Sections Obtained with Monoenergetic Photons," Lawrence Livermore Laboratory report UCRL-78482 (1976).

14. D. G. Madland and J. R. Nix, "Calculation of Prompt Fission Neutron Spectra," Proc. Int. Conf. on Nuclear Cross Sections for Technology, Knoxville, TN (Oct. 1979).

15. P. G. Young and E. D. Arthur, "GNASH: A Preequilibrium, Statistical Nuclear-Model Code for Calculation of Cross Sections and Emission Spectra," Los Alamos Scientific Laboratory report LA-6947 (1977).

16. D. C. Dodder, G. M. Hale, and K. Witte, "EDA, An Energy Dependent Analysis Code," unpublished.

17. C. Kalbach and F. Mann, personal communication.

18. E. D. Arthur and P. G. Young, "Evaluation of Neutron Cross Sections on Iron Between 1 and 40 MeV," Proc. Int. Conf. on Nuclear Cross Sections for Technology, Knoxville (Oct. 1979).

19. R. Roussin, Oak Ridge National Laboratory, personal communication.

20. R. J. Barrett and R. E. MacFarlane, "Coupled Neutron and Photon Cross Sections for Transport Calculations," Los Alamos Scientific Laboratory report LA-7808-MS (April 1979).

21. R. J. LaBauve, T. R. England, D. C. George, and M. G. Stamatelatos, "The Application of a Library of Processed ENDF/B-IV Fission Product Aggregate Decay Data in the Calculation of Decay-Energy Spectra," Los Alamos Scientific Laboratory report LA-7483-MS (Sept. 1978).

22. R. J. LaBauve, D. C. George, and T. R. England, "FITPULS, A Code for Obtaining Analytic Fits to Aggregate Fission-Product Decay Energy Spectra," Los Alamos Scientific Laboratory report LA-8277-MS (March 1980).

23. R. Roussin, Oak Ridge National Laboratory, personal communication.

24. G. Erdtman and W. Soyka, "The Gamma Rays of Radionuclides: Tables for Applied Gamma Ray Spectrometry," Verlag Chemie, Weinheim, New York (1979).

25. W. Walker, Atomic Energy of Canada, LTD, personal communication of preliminary actinide data (Nov. 1979).

26. A. Tobias, Berkeley Nuclear Laboratories, U. K., and A. Nichols, AEE, Winfirth, personal communication of preliminary actinide data (Oct. 1979).

27. F. W. Walker, G. J. Kirouac, and F. M. Rourke, Chart of the Nuclides, Twelfth Edition (General Electric Co., Knolls Atomic Power Laboratory, Schenectady NY, 1977).

28. C. M. Lederer and V. S. Shirley, Eds. Table of Isotopes, Seventh Edition (John Wiley and Sons, Inc. NY, 1978).

29. M. G. Stamatelatos and T. R. England, "Accurate Approximations to Average Beta-Particle Energies and Spectra," Nucl. Sci. Eng. 63, 204 (1977).

Printed in the United States of America. Available from
National Technical Information Service
US Department of Commerce
5285 Port Royal Road
Springfield, VA 22161

Microfiche $3.00

001-025	4.00	126-150	7.25	251-275	10.75	376-400	13.00	501-525	15.25
026-050	4.50	151-175	8.00	276-300	11.00	401-425	13.25	526-550	15.50
051-075	5.25	176-200	9.00	301-325	11.75	426-450	14.00	551-575	16.25
076-100	6.00	201-225	9.25	326-350	12.00	451-475	14.50	576-600	16.50
101-125	6.50	226-250	9.50	351-375	12.50	476-500	15.00	601-up	

Note: Add $2.50 for each additional 100-page increment from 601 pages up.